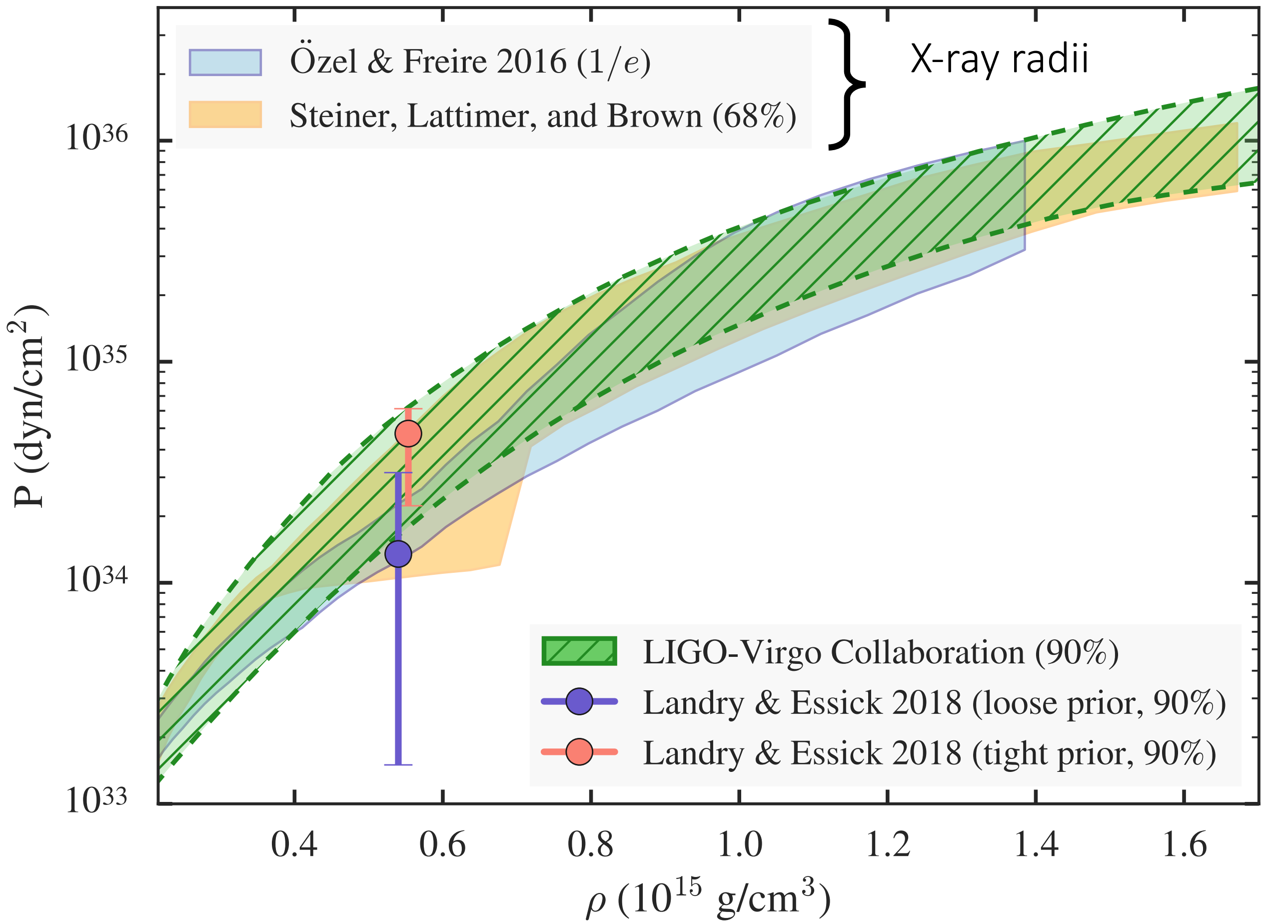

Neutron Stars and Dense Matter Equation of State

Feryal Ozel
University of Arizona

Cold Dense Matter EoS is a Hard Problem

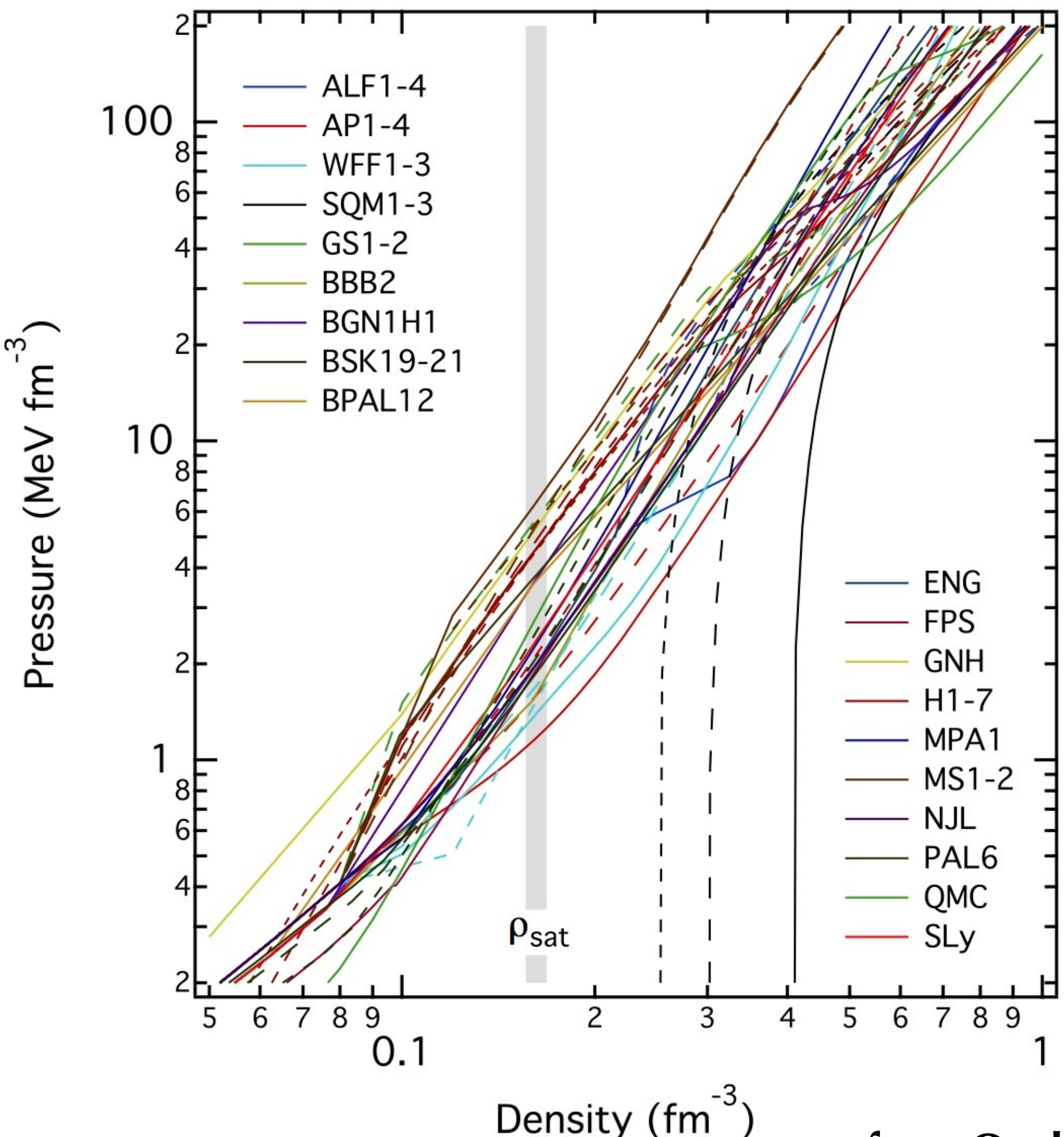

from Ozel & Freire 2016, ARAA

Neutron Star Observations Can Pin Down EoS

EoS maps directly to macroscopic properties of neutron stars
and vice versa

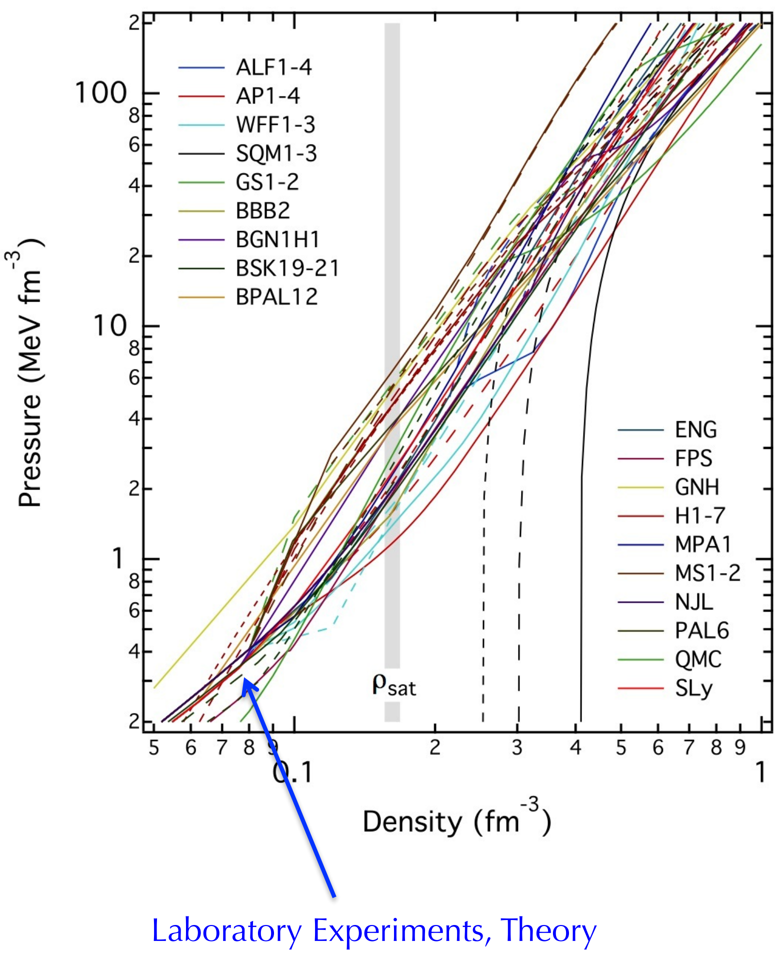

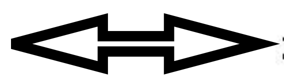

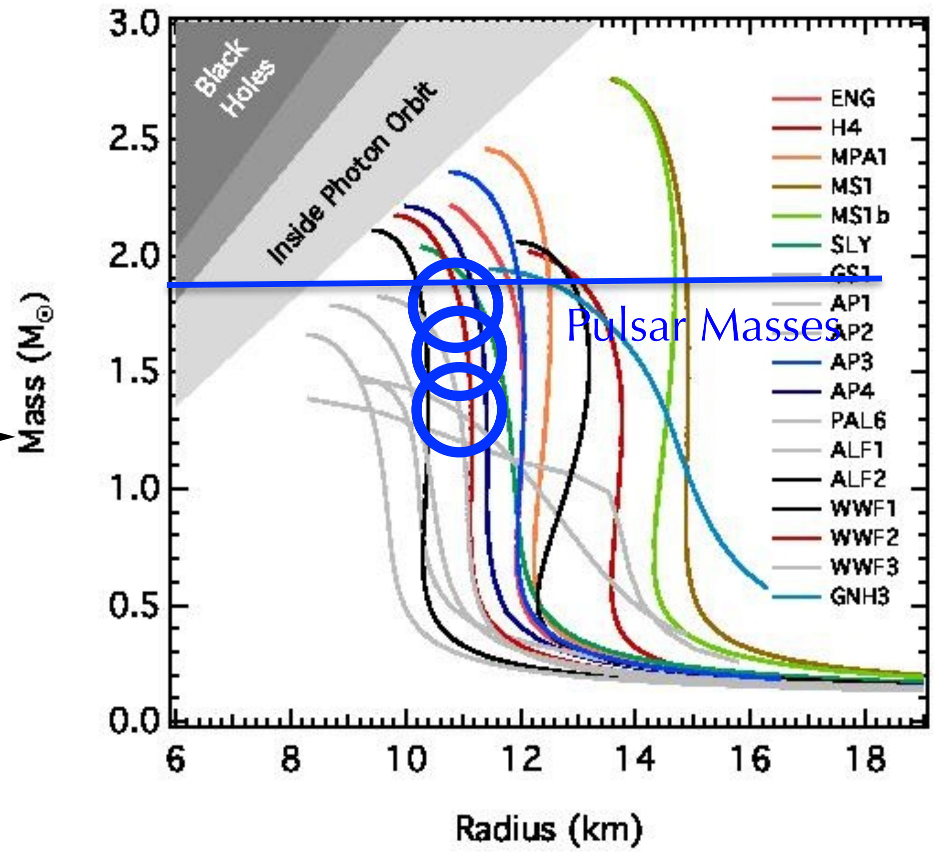

Lattimer & Prakash 2001; Ozel & Psaltis 2009

Probes of the NS EoS

- Pulsar masses
- Neutron Star Radii from X-rays (2 methods)
- Gravitational Wave Signals

upcoming:

- Moment of Inertia

Measuring Neutron Star Masses

$$f = \frac{(M_{\rm c} \sin i)^3}{M_{\rm T}^2} = \frac{4\pi^2}{T_\odot} \frac{x_{\rm PSR}^3}{{P_b}^2},$$

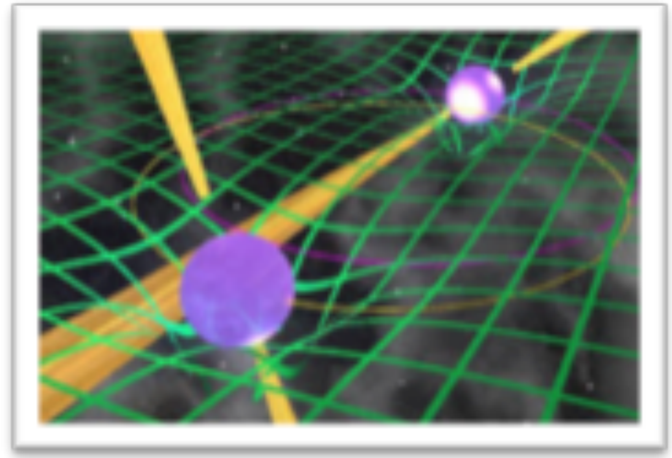

$$\dot{\omega} = 3 \left(\frac{P_b}{2\pi}\right)^{-5/3} (T_\odot M_{\rm T})^{2/3} \left(1 - e^2\right)^{-1}$$

Advance of periastron

$$\gamma = e \left(\frac{P_b}{2\pi}\right)^{1/3} T_\odot^{2/3} M_{\rm T}^{-4/3} M_{\rm c} \left(M_{\rm PSR} + 2M_{\rm c}\right)$$

Einstein delay

$$r = T_\odot M_{\rm c},$$

Shapiro delay r

$$s = \sin i = x_{\rm PSR} \left(\frac{P_b}{2\pi}\right)^{-2/3} T_\odot^{-1/}$$

Shapiro delay s

$$\dot{P}_b = -\frac{192\pi}{5} \left(\frac{P_b}{2\pi T_\odot}\right)^{-5/3} \left(1 + \frac{73}{24} e^2 + \frac{37}{96} e^4\right) \times (1 - e^2)^{-7/2} M_{\rm PSR} M_{\rm c} M_{\rm T}^{-1/3}$$

Orbital period decay

Masses from Post-Keplerian Parameters

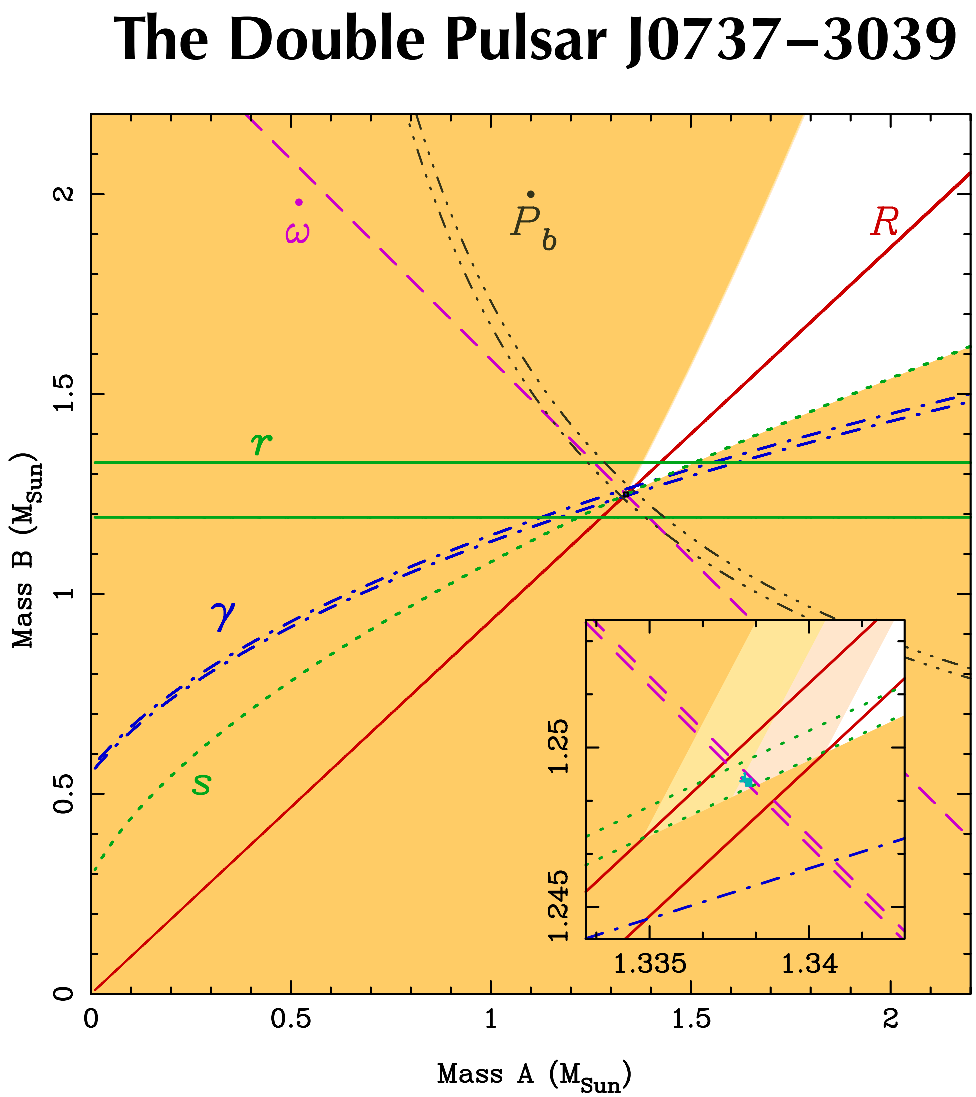

Lyne et al. 2004
Kramer & Wex 2009

Record Holders in Mass

— $1.92 \pm 0.04\ M_\odot$ (Fonseca et al. 2016; Pulsar timing)

— $2.04 \pm 0.04\ M_\odot$ (Antoniadis et al. 2013; Pulsar timing+WD Spectroscopy)

— $2.14_{-0.09}^{+0.10}$ (Cromartie et al. 2020; Pulsar timing)

Measurement of Neutron Star Radii

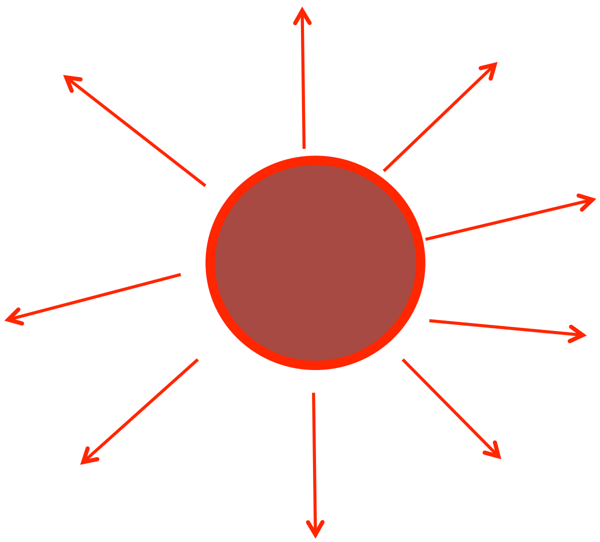

Method I: Spectroscopy of Surface Emission

$$R^2 = \frac{F\ D^2}{\sigma\ T^4}\left(1 - \frac{2GM}{Rc^2}\right)^{-1}$$

Uses Models of Neutron Star Atmospheres and Spacetimes

Radius Measurements: Neutron Star in a Binary

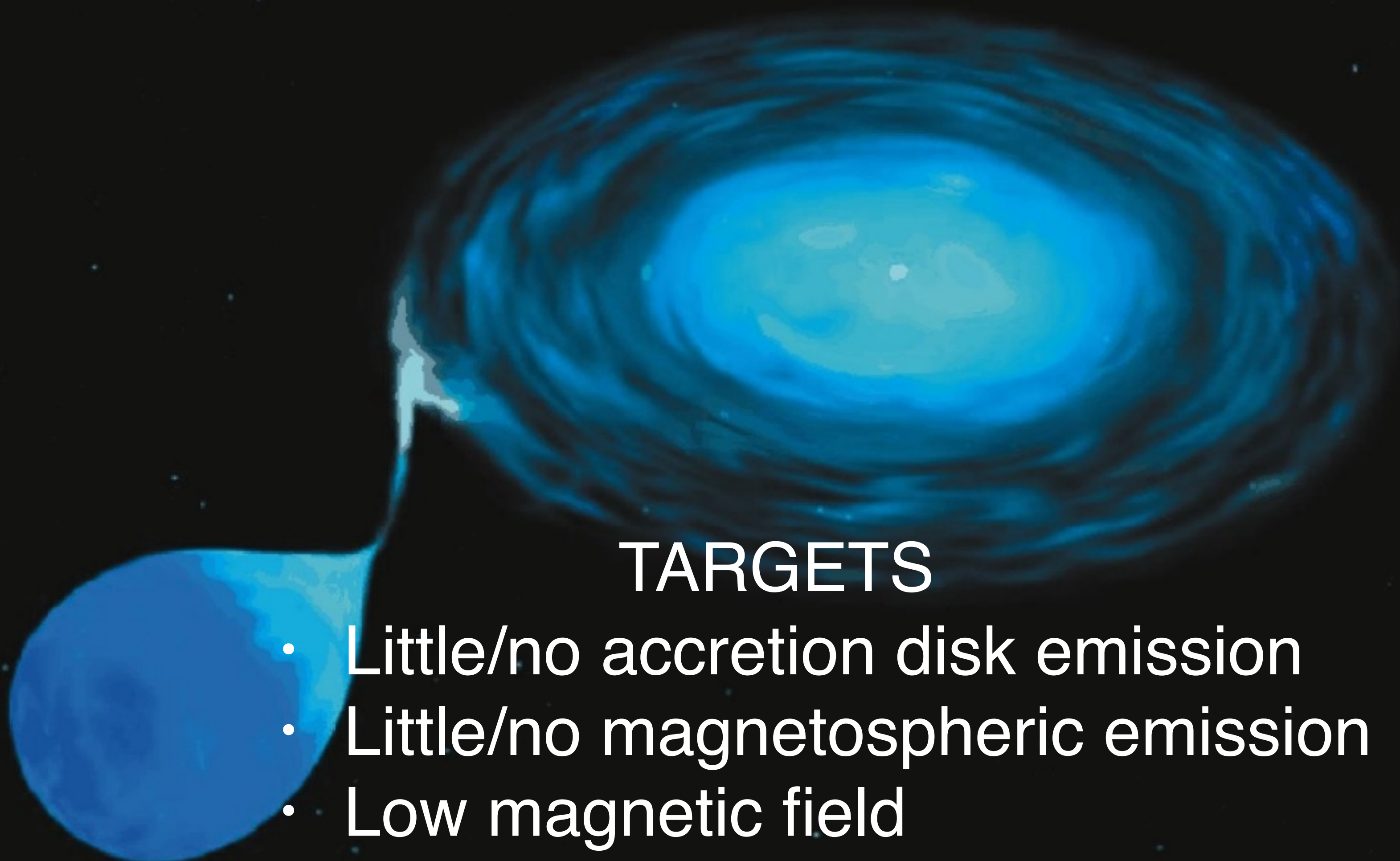

TARGETS

- Little/no accretion disk emission
- Little/no magnetospheric emission
- Low magnetic field
- Thermal emission observed in quiescence and in thermonuclear bursts

Radius Measurement using Thermonuclear Bursts

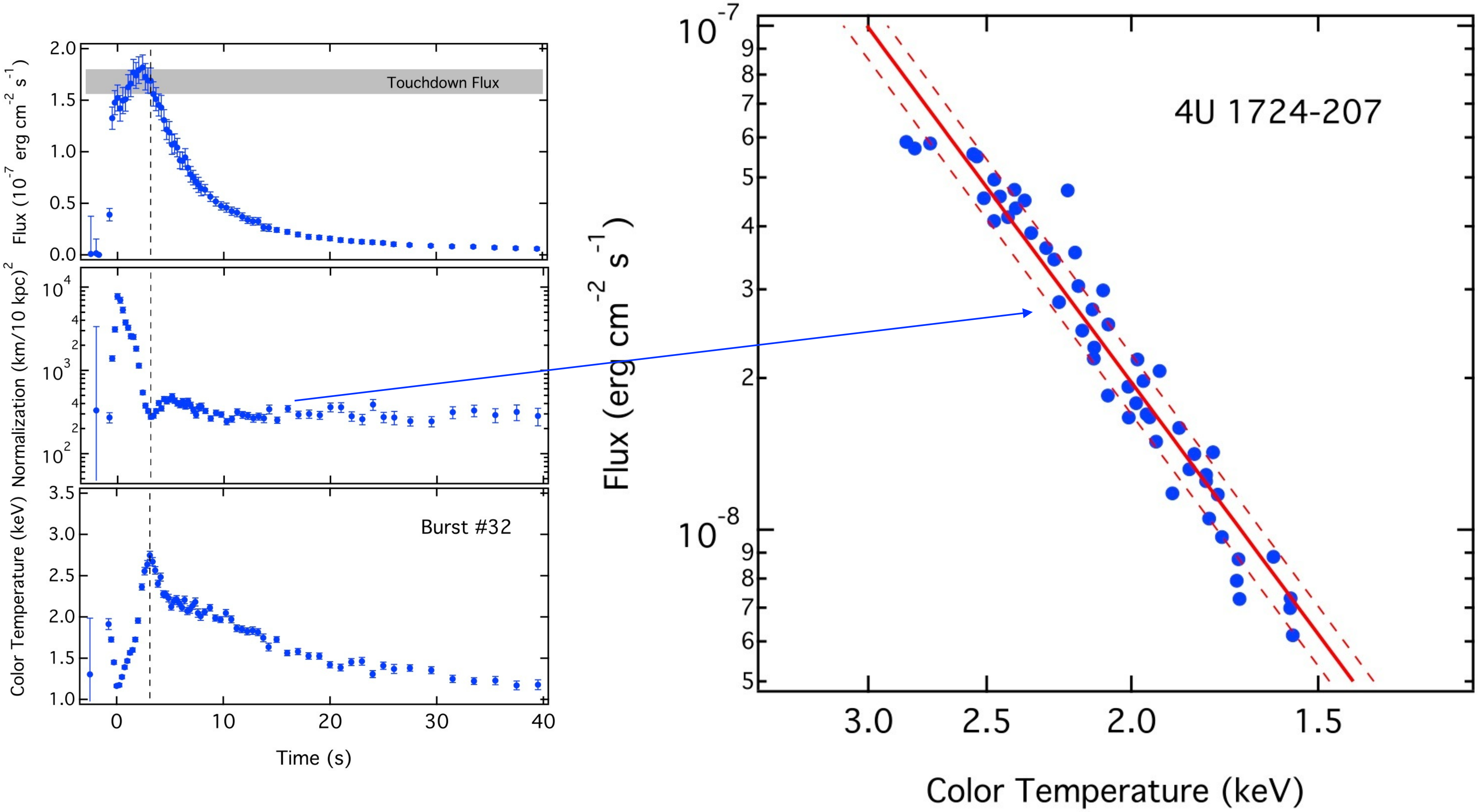

Guver et al. 2012 a,b

Radius Measurement using Thermonuclear Bursts

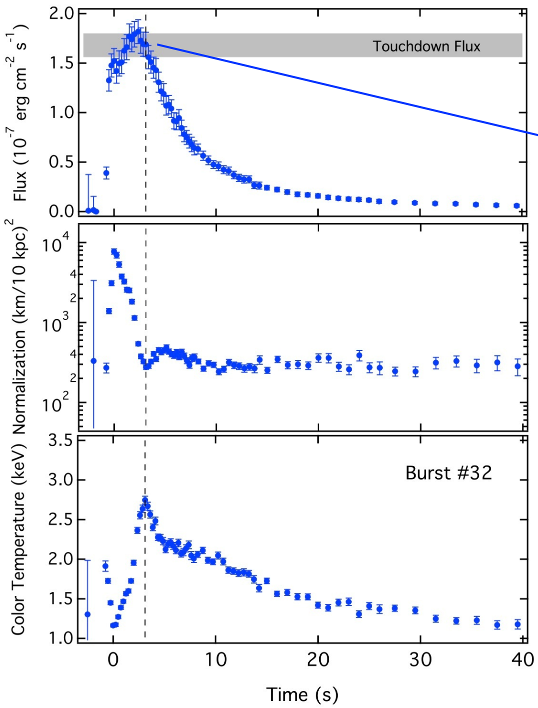

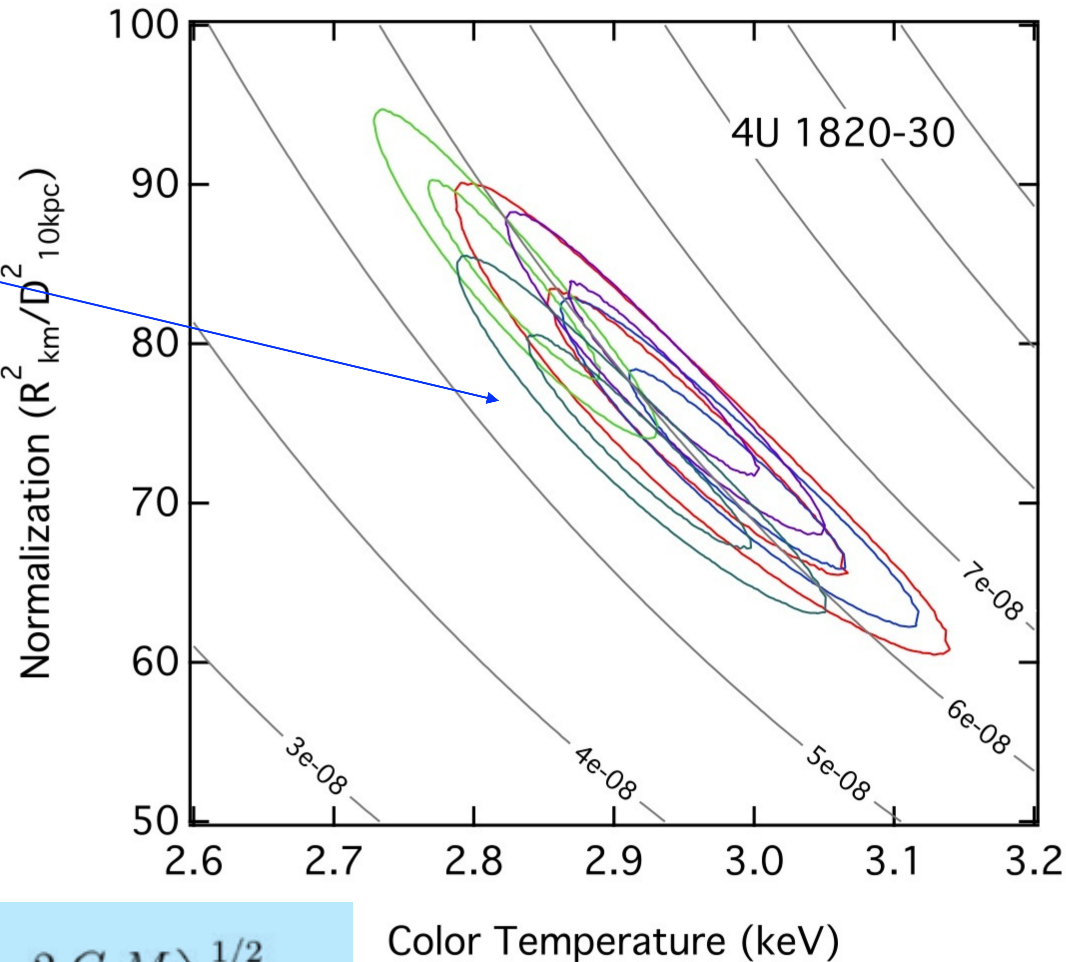

$$L_{\mathrm{Edd}} = \frac{4\,\pi\,G\,c\,M}{\sigma_T\,(1+X)}\left(1-\frac{2\,G\,M}{R\,c^2}\right)^{1/2}$$

Guver et al. 2012 a,b

Six Burst Sources

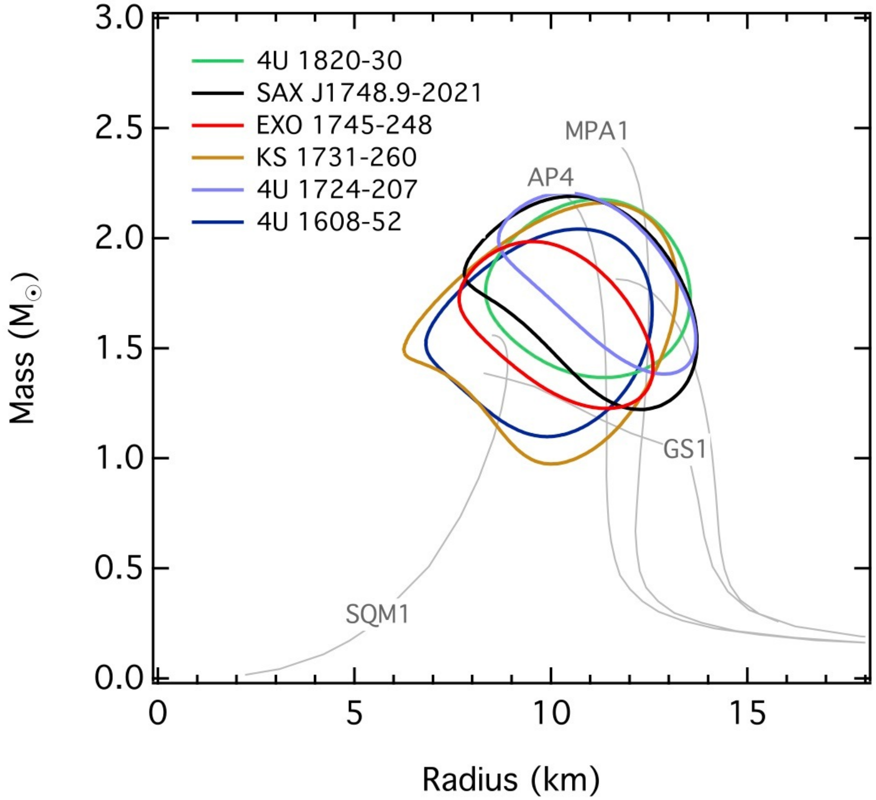

Eight Quiescent Sources

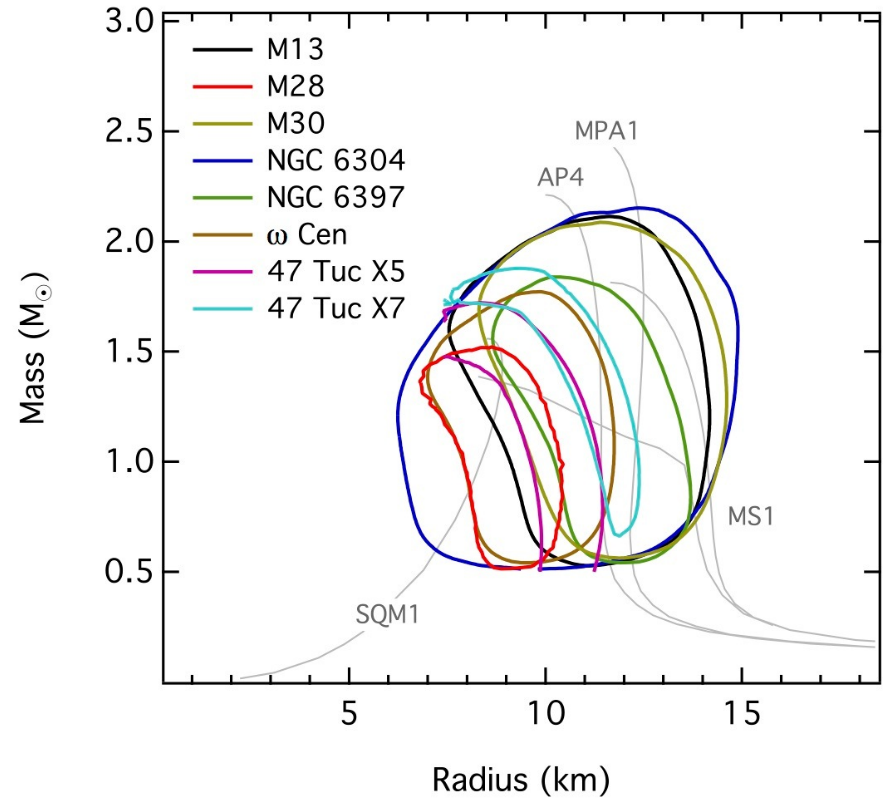

Ozel et al. 2016

Ozel et al. 2009, 2010, Steiner et al. 2010, 2013, Guver et al. 2012 a,b, Guillot et al. 2013, Heinke et al. 2014, Baubock et al. 2015, Ozel & Psaltis 2015, Bogdanov et al. 2016, Ozel& Freire 2016, Steiner et al. 2017

Neutron Star Radius Results from Method I

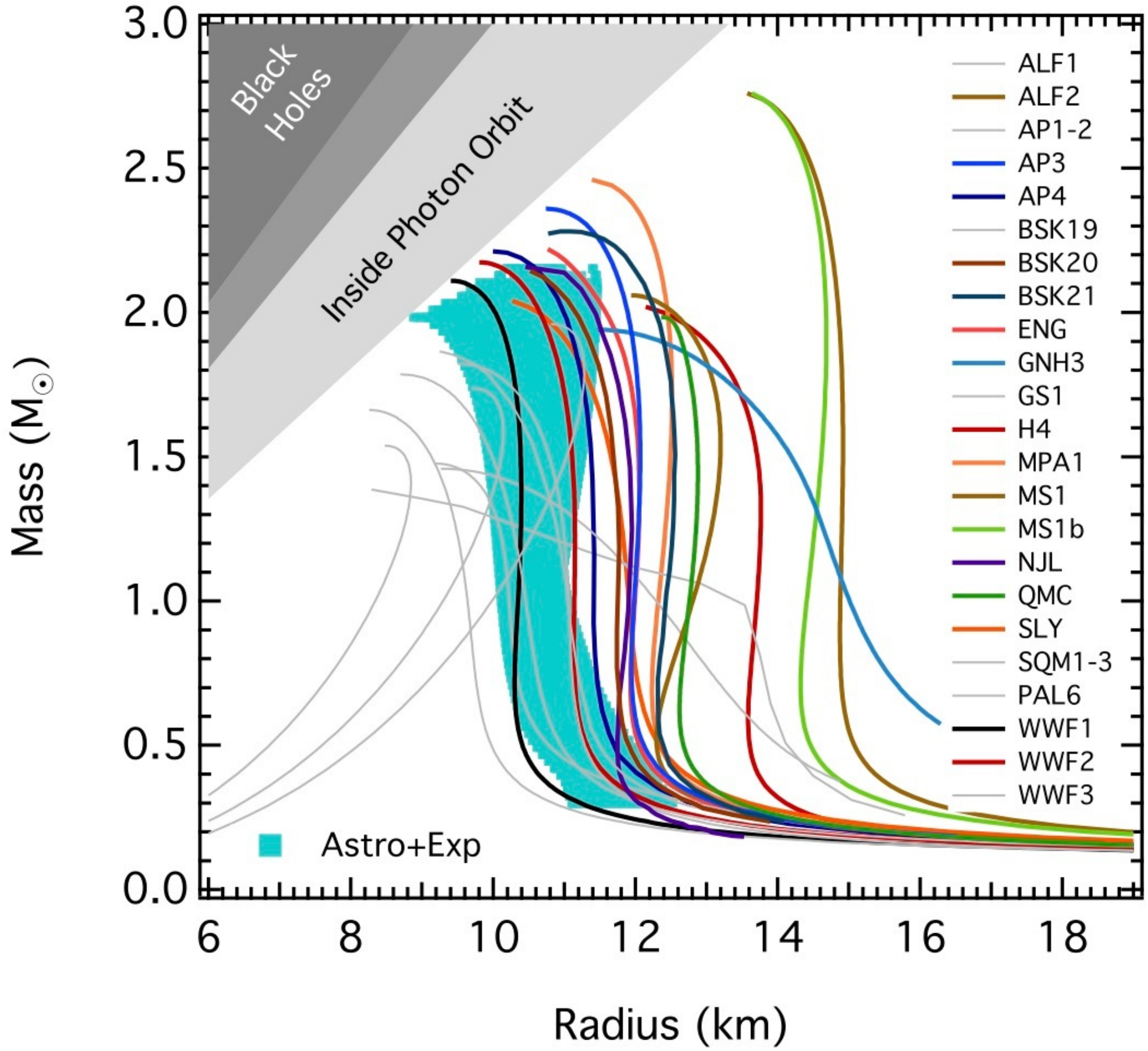

Ozel et al. 2016

Radii are 10-11.5 km, 95% C.I.

Implies $M_{max} \sim 2.05\ M_\odot$

Equation of State Results from Method I

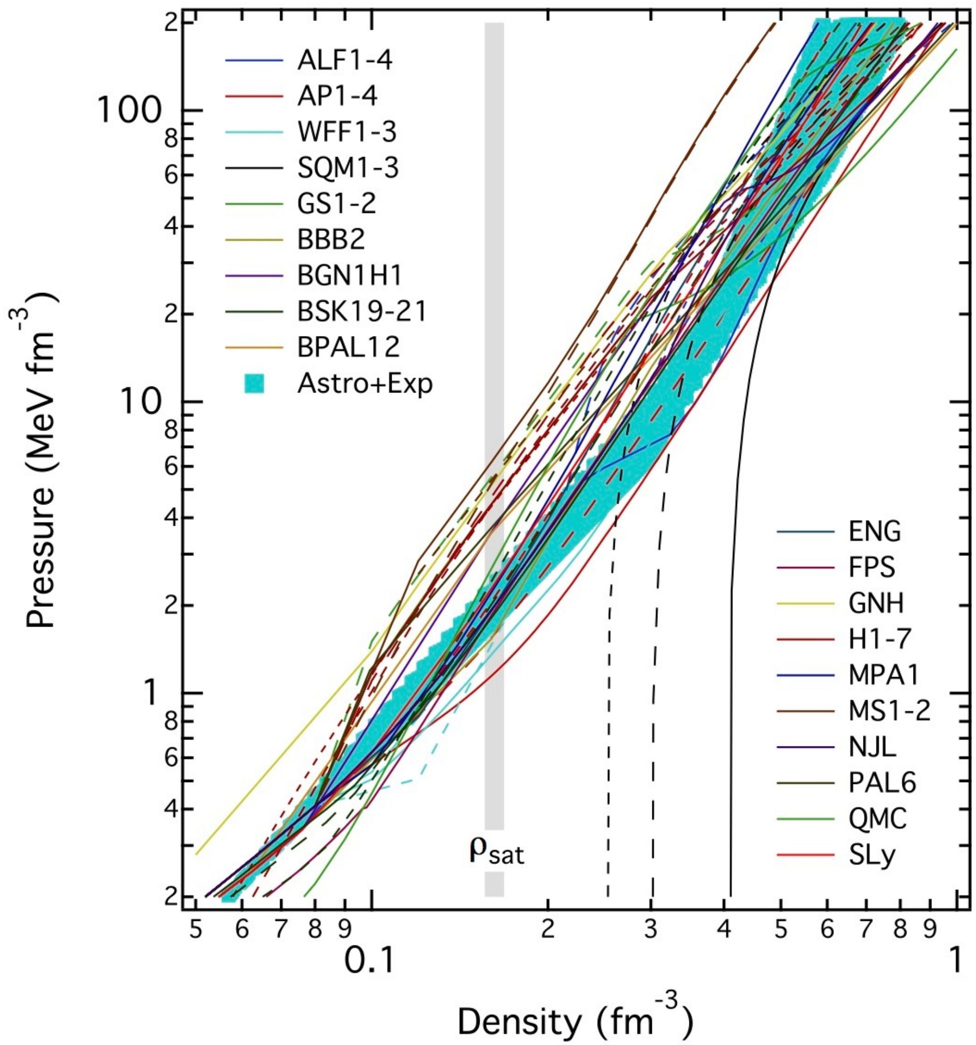

Dense Matter EoS is soft, i.e., lower pressure than some nucleonic models at intermediate densities

May indicate new (quark?) degrees of freedom

Implies low isospin symmetry energy

Ozel et al. 2016

Not a settled problem

The effect of accretion on the measurement of neutron star mass and radius in the low-mass X-ray binary 4U 1608−52

Juri Poutanen,[1,2⋆] Joonas Nättilä,[1,2] Jari J. E. Kajava,[3,4,2] Outi-Marja Latvala,[2]
Duncan Galloway,[5,6] Erik Kuulkers[3] and Valery Suleimanov[7,8]

We analyse the hard-state burst to put the lower limit on the neutron star radius in 4U 1608–52 of 13 km (for masses 1.2–2.4 $M_{\odot}$). The best agreement with the theoreti-

Radius Measurement Method II: Pulse Profile Modeling

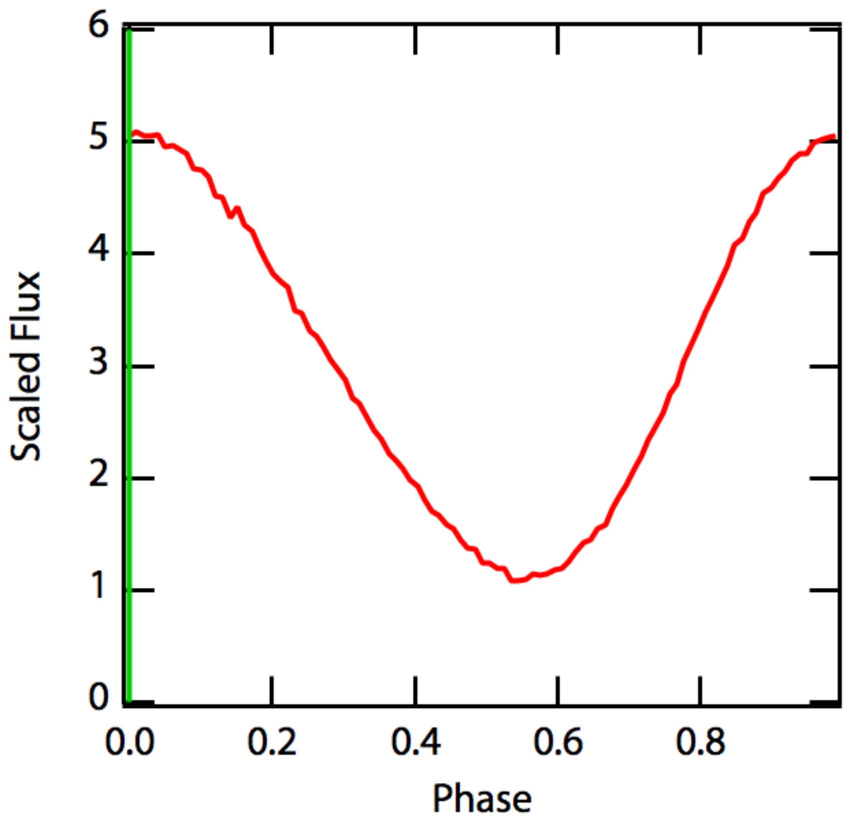

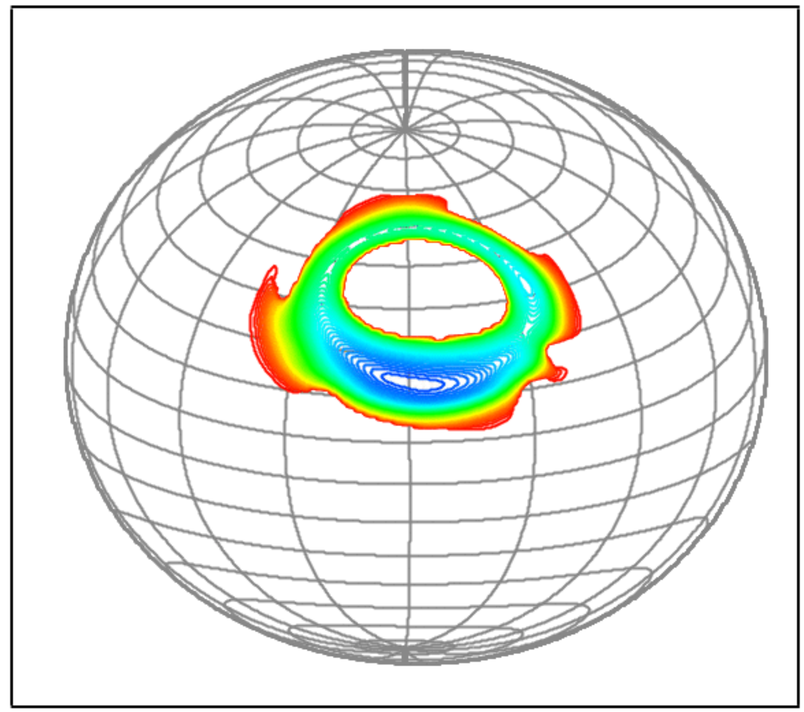

Weinberg, Miller, & Lamb 2000; Bogdanov et al. 2007, 2013; ; Baubock et al. 2015, 2016, Psaltis, Ozel, Chakrabarty 2014

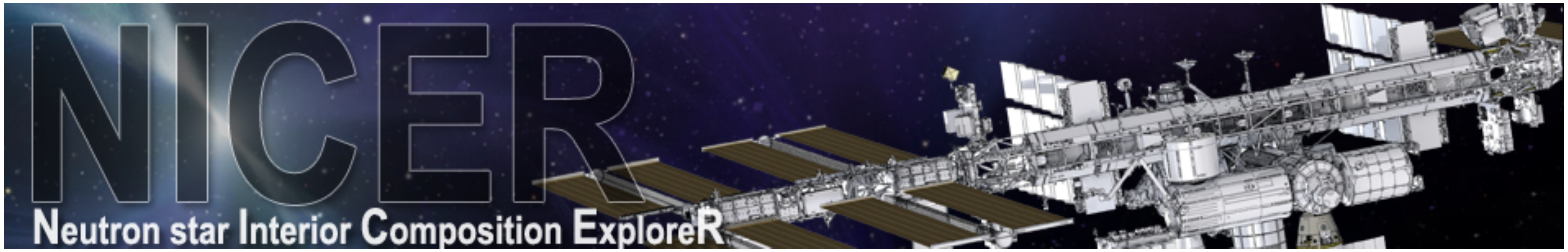

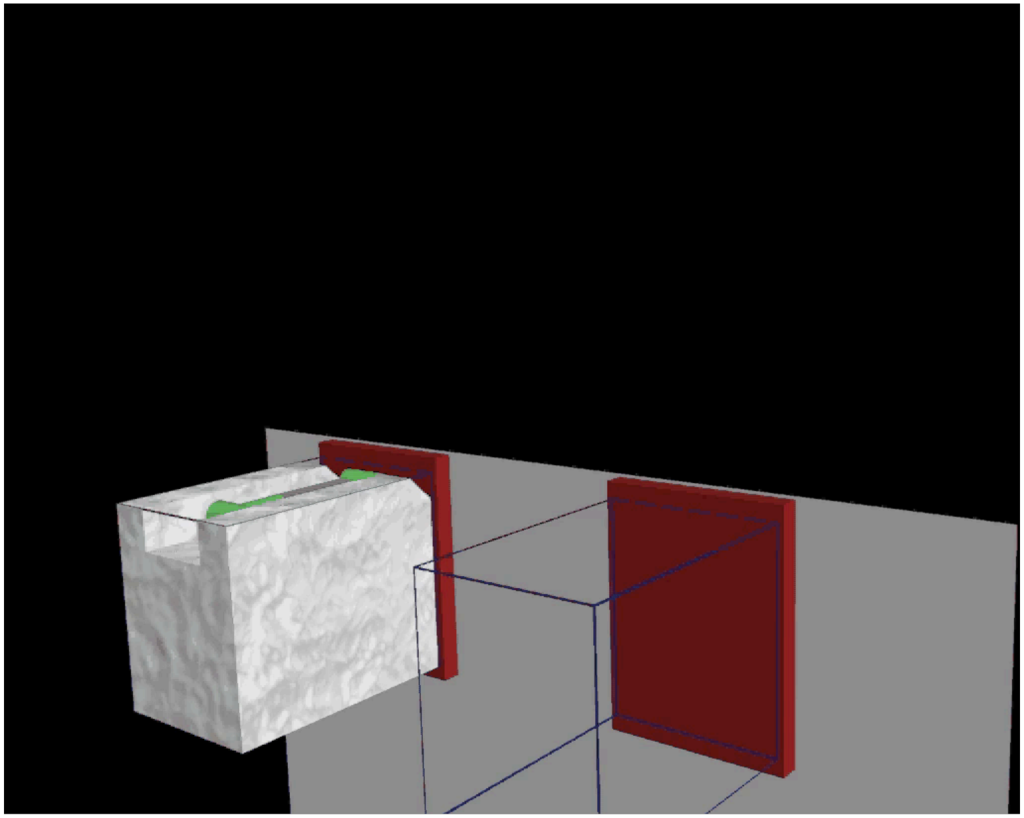

Launched: May 2017

Collecting data on key pulsar targets
thermonuclear bursts

First Analyses from NICER data

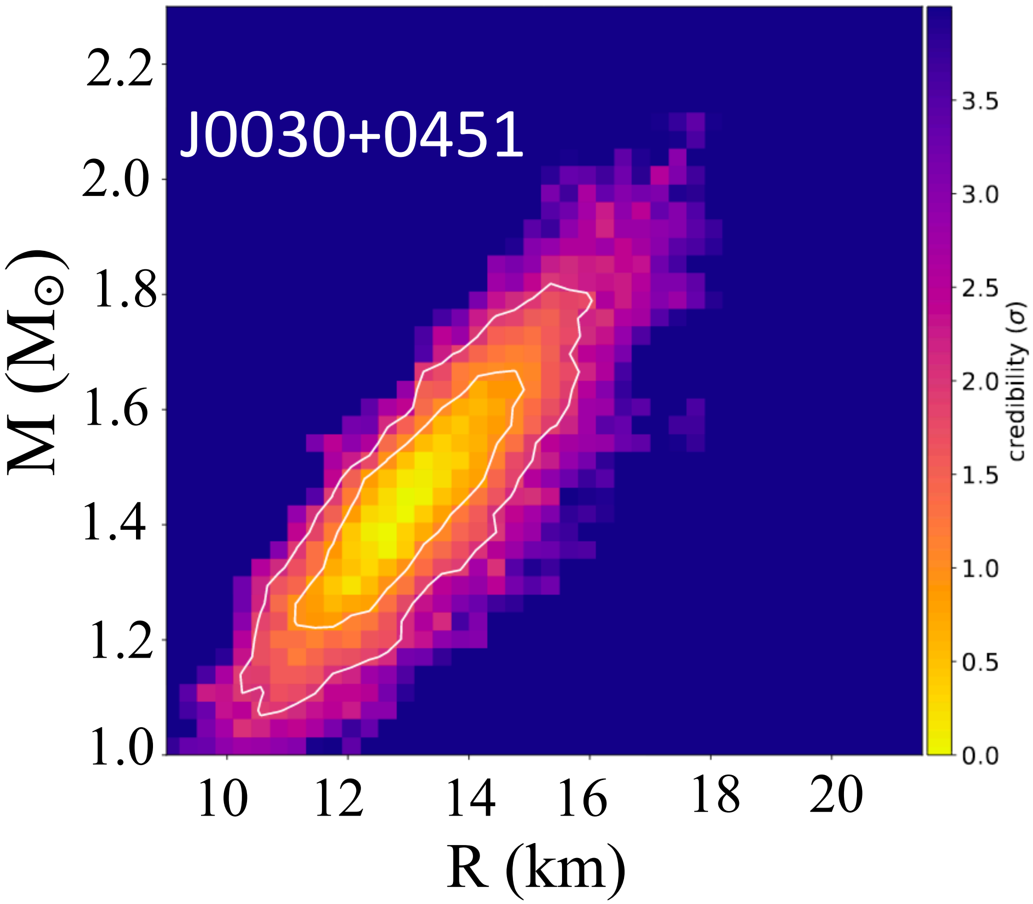

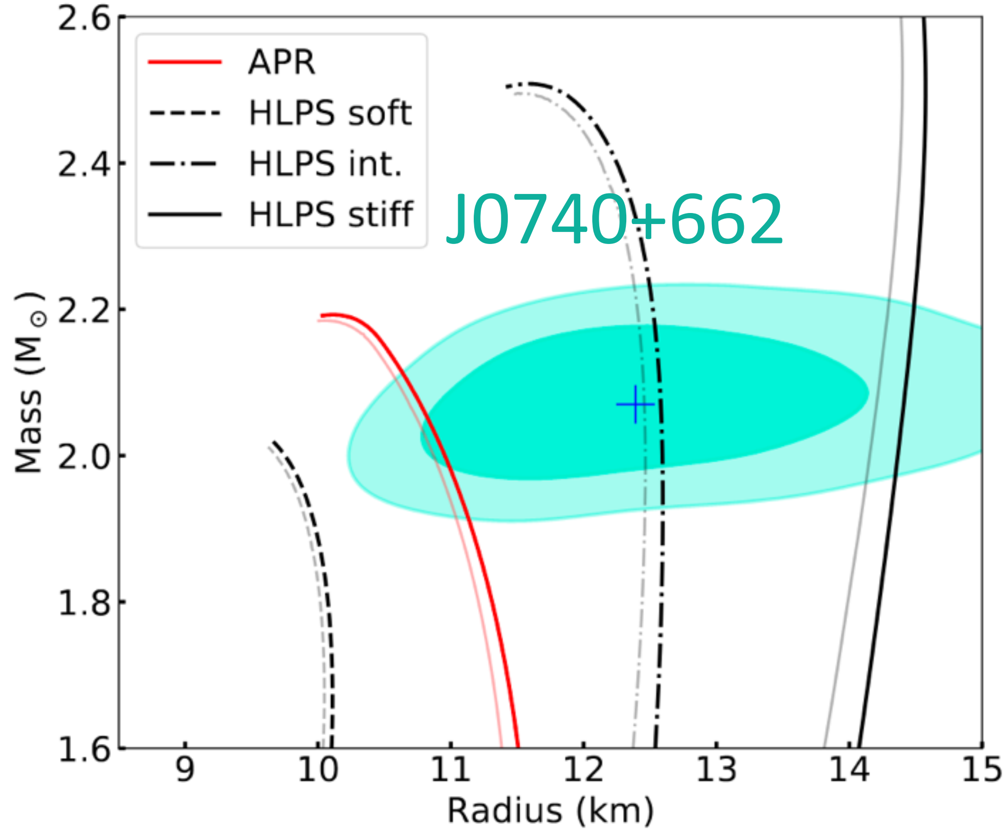

Riley et al. 2019, 2021
Miller et al. 2019, 2021

Questions and Systematics with NICER Results

Very large number of free parameters (size, shape, & latitude of each spot, observer's inclination, beaming function of radiation, background, foreground, …)

Spot distributions not physically motivated

Impact of bombardment on polar caps (as opposed to the deep heating model assumed in the analyses)

Subtraction of the magnetospheric component (assumed a power-law)

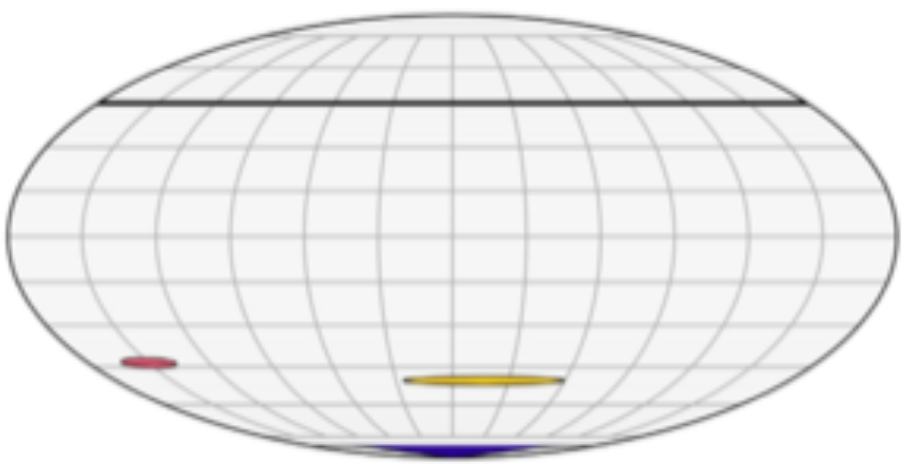

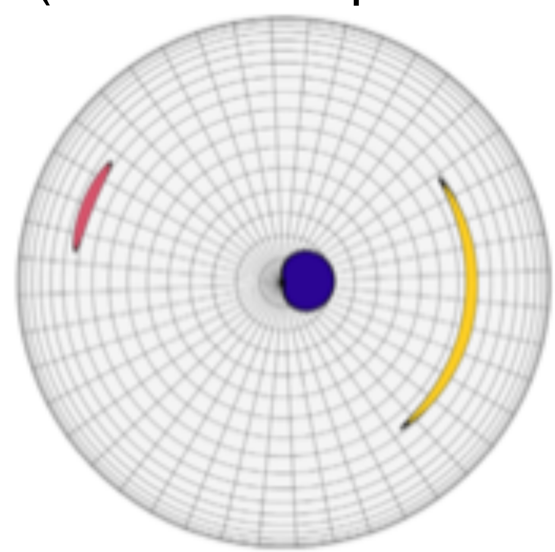

Tidal deformability from GW170817

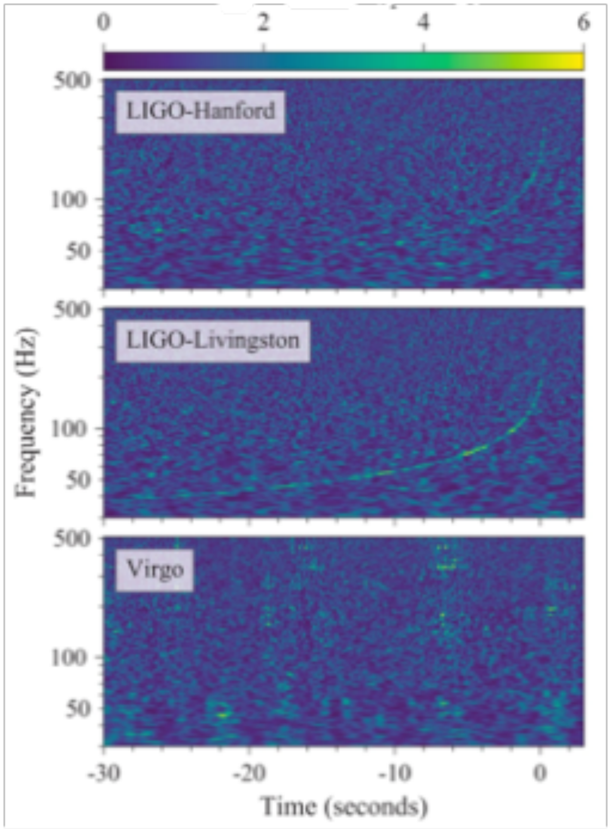

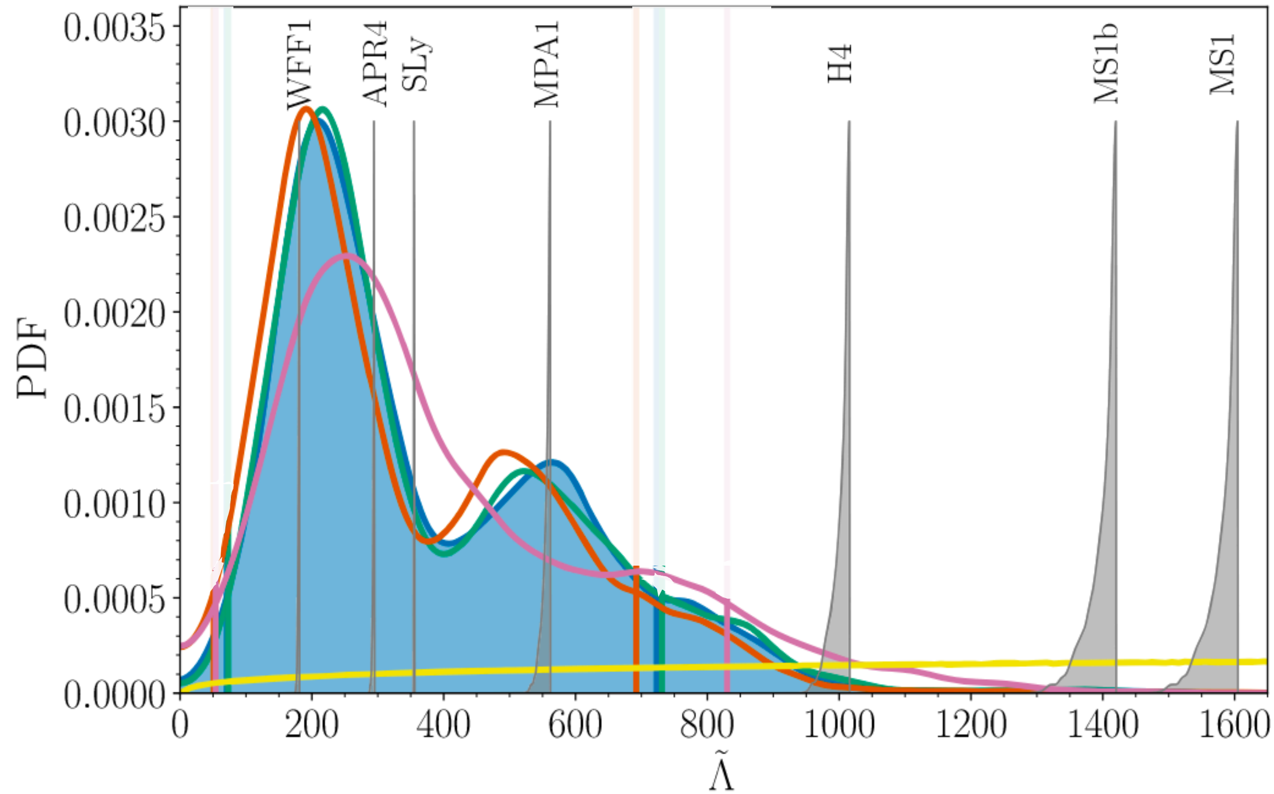

LVC (2017, 2019)

From analysis of binary waveform, one can extract *effective* (or *binary*) tidal deformability:

$$\widetilde{\Lambda} = \frac{16}{13}\frac{(m_1 + 12m_2)m_1^4\ \Lambda_1 + (m_2 + 12m_1)m_2^4\ \Lambda_2}{(m_1 + m_2)^5}$$

New Universal Mapping Between $\tilde{\Lambda}$ and Stellar Radius

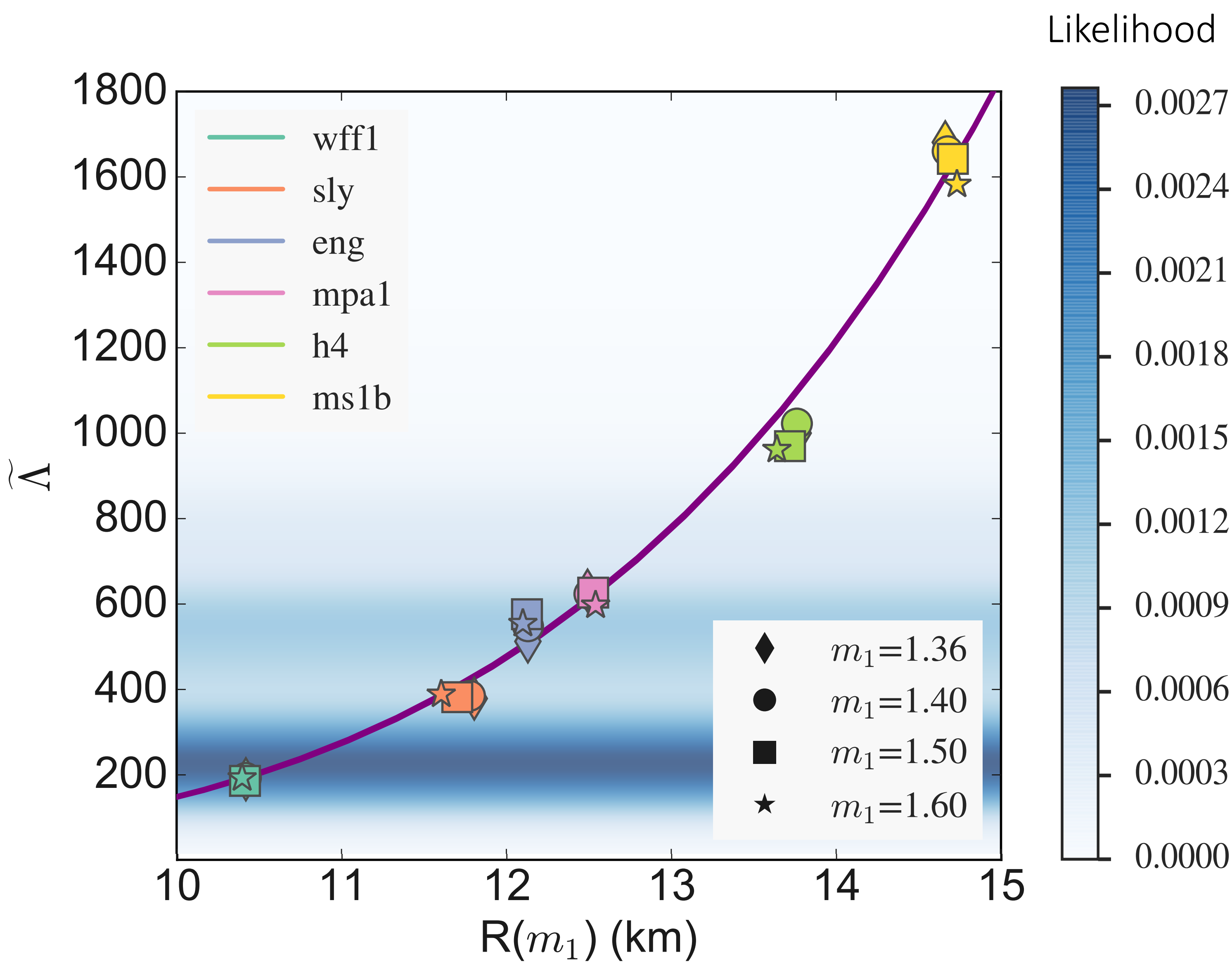

Raithel, Özel, and Psaltis (2018); Raithel (2019).

Connecting tidal deformability to stellar radius

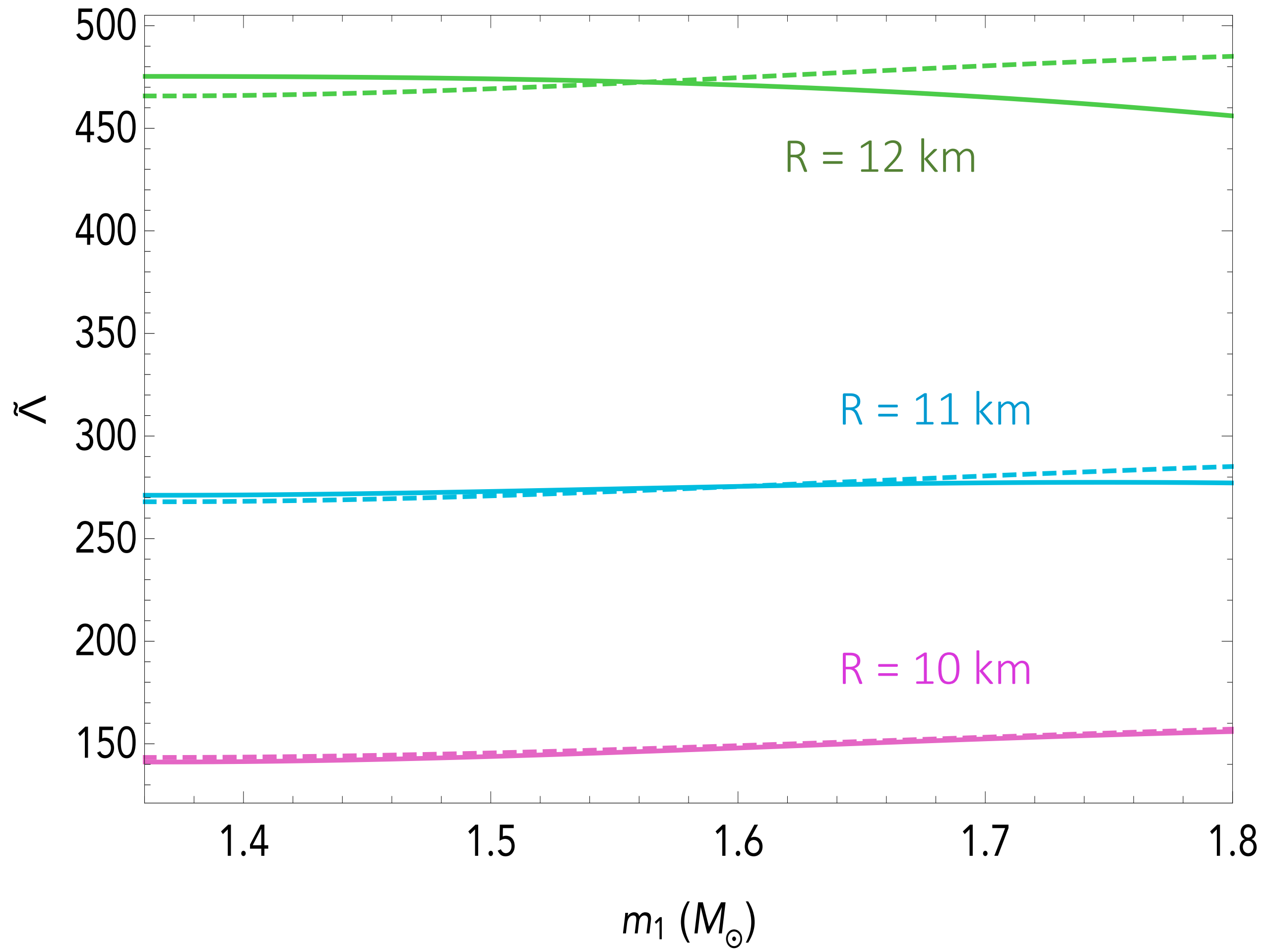

$\tilde{\Lambda}$ no longer depends on individual component masses when M_c is fixed

Raithel, Özel, and Psaltis (2018)

Neutron star radii from GW and X-ray measurements

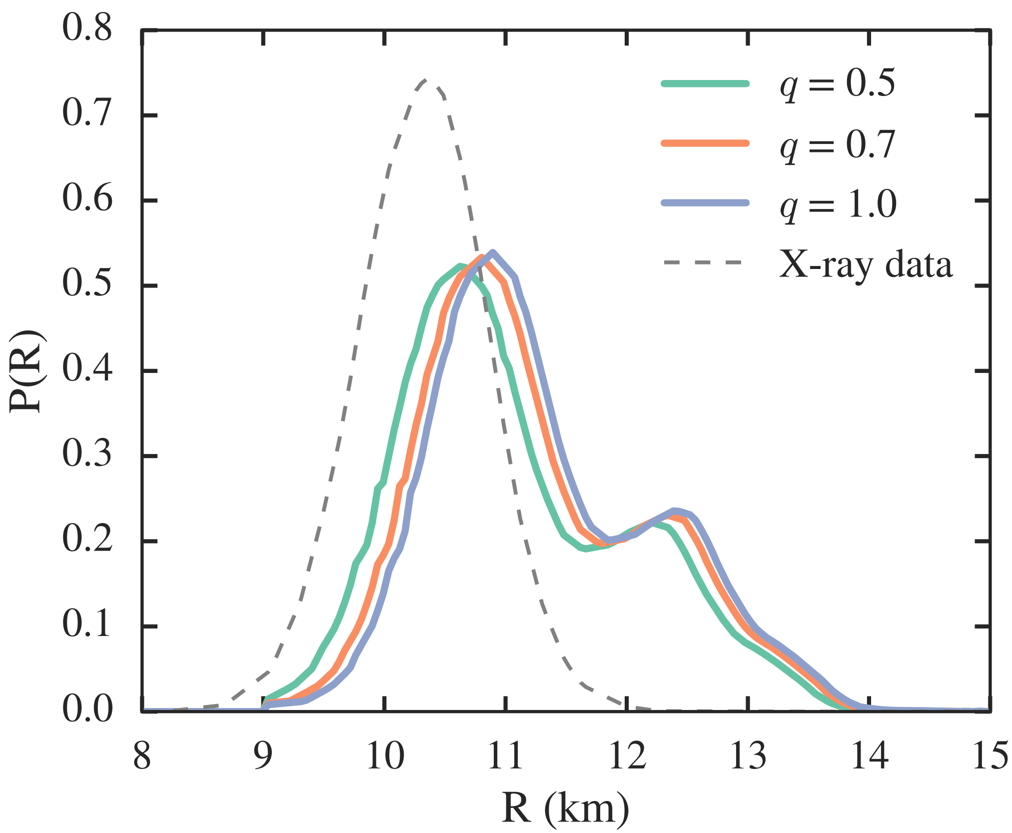

Raithel (2019); Raithel, Özel, and Psaltis (2021).
X-ray data from LMXB analysis of Özel+ 2016.

$$P(R) = P(\widetilde{\Lambda})\left|\frac{\partial \widetilde{\Lambda}}{\partial R}\right|$$

$R_{GW170817}$ = 10.2 – 11.7 km
(68% HPD interval)

- See also De et al. (2018) and Zhao & Lattimer (2018) for similar $\widetilde{\Lambda}(R)$ relationship, with different set of assumptions.
- And see Annala+ (2018), Abbott+ (2018), Most+ (2018), Tews+ (2018), Lim and Holt (2018), … for many more estimates of R from GW170817

Where We Are

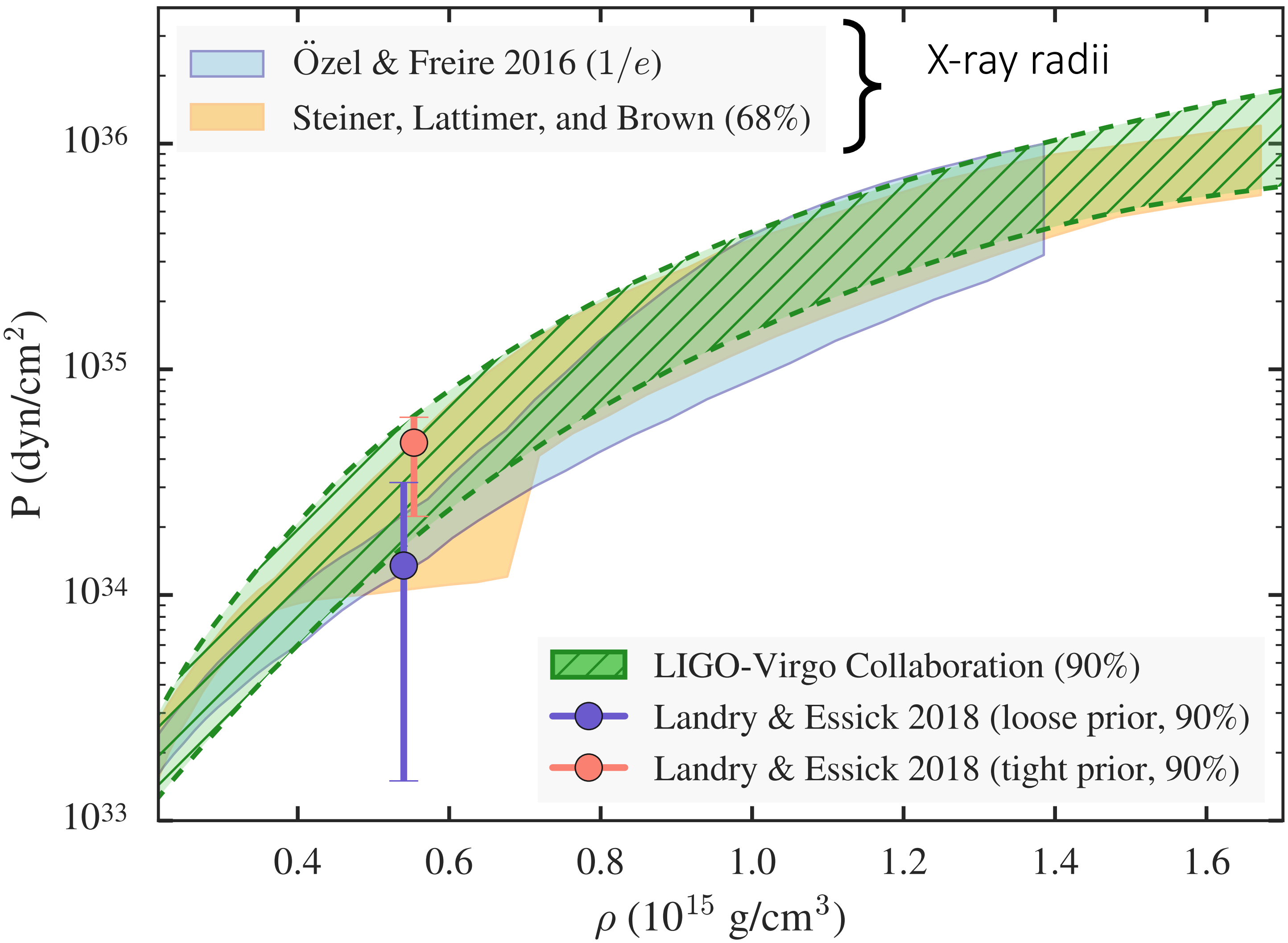

Özel & Freire 2016 (1/e)
Steiner, Lattimer, and Brown (68%)
X-ray radii
LIGO-Virgo Collaboration (90%)
Landry & Essick 2018 (loose prior, 90%)
Landry & Essick 2018 (tight prior, 90%)
P (dyn/cm²)
ρ (10¹⁵ g/cm³)
10³⁶
10³⁵
10³⁴
10³³
0.4
0.6
0.8
1.0
1.2
1.4
1.6